Journal of Clinical and Medical Images

Case Report

ISSN: 2640-9615 | Volume 6

Vertical Multiphoton Imaging of Human Skin *in vivo*

Hans Georg Breunig[1*], Ana Batista[1], Karsten König[1,2]

[1]JenLab GmbH, Johann-Hittorf-Str. 8, 12489 Berlin, Germany

[2]Department of Biophotonics and Laser Technology, Saarland University, 66123, Saarbrücken, Germany

[*]Corresponding author:

Karsten König,
Saarland University, Department of Biophotonics and Laser Technology, Campus A5.1, 66123 Saarbruecken, Germany,
E-mail: k.koenig@blt.uni-saarland.de

Received: 21 Sep 2022
Accepted: 01 Oct 2022
Published: 07 Oct 2022
J Short Name: JCMI

Keywords:

Autofluorescence; *In vivo* imaging; Histopathology; Skin imaging; Multiphoton tomography

Citation:

Breunig et al., Vertical Multiphoton Imaging of Human Skin in vivo. J Clin Med Img. 2022; V6(17): 1-7

1. Abstract

Histopathology of skin biopsies is invaluable for the diagnosis of skin conditions. However, it is an elaborate and time-consuming procedure whose diagnostic yield depends on the experience of highly trained experts. In contrast, optical imaging methods can non- invasively provide in vivo images but, mostly, do not fulfill the current clinical need for an imaging tool which images the skin vertically with high resolution while offering at the same time large histopathological-like contrast. Multiphoton tomography (MPT) provides sufficient subcellular resolution and additional metabolic information based on fluorescence lifetime imaging (FLIM). So far, MPT is mainly used to provide horizontal "en-face" optical sections. Here, we report on vertical multiphoton skin imaging that can close the gap between in vivo optical biopsies and histopathology. Vertical images were obtained by synchronizing the movement of a galvo-scanning mirror with adjustments of the distance between skin and focusing optics. Horizontal and vertical multiphoton skin biopsies offer information on the microscopic skin anatomy and cell architecture including pathological modifications which can be derived straightforwardly in vivo within seconds. These in vivo images are compared with images of histopathologically prepared human skin samples. Benefits as well as drawbacks of vertical MPT are discussed.

2. Introduction

Histopathology, the current gold standard in anatomical pathology for the analysis and diagnosis of skin conditions, involves several preparation steps like tissue removal, fixation, and sectioning as well as one or more staining procedures of the processed histology slides [1]. A sample is then evaluated with optical microscopy by highly trained experts. For an exact diagnosis of skin conditions such an elaborate effort is often necessary. The medical diagnosis, for example for cancer, is based on the histological findings and the opinion of the pathologist [2, 3]. However, in many cases, which includes further applications besides diagnosis, such a highly-detailed view as provided by histopathology is not needed or a quick supplement or pre-assessment to clinical diagnosis is desired. Furthermore, the supply of human skin for research purposes is limited and the costs and demands of histopathological examinations too demanding such that substitute measures are employed. For example, in areas of research such as analysing the effects of radiation, transdermal-drug delivery, screening of the toxicity and penetration of topically applied compounds or for studying wound repair often alternatives like animal skin, *in vitro* cultured skin phantoms, and biosynthetic skin substitutes are used. Whether or not results obtained with these substitutes can be directly applied to human in vivo skin is a topic of an on-going discussion and often put into question [4, 5]. Both demands, (I) a fast and uncomplicated, nevertheless, highly detailed view, which make histopathologic examination unnecessary, and (II) true in vivo human skin investigations, maybe fulfilled by non-invasive optical methods [2]. In particular, multiphoton tomography (MPT) offers a fast and cost- effective, alternative by providing a unique microscopic view into human skin in vivo based on endogenous fluorescence and other signals without the need of staining or elaborate preparation procedures [6]. With MPT, the time required for evaluation of the human skin is reduced to a few minutes rather than several hours or days. It is well known that the nonlinear signal dependence on the excitation-light intensity results in an intrinsic three-dimensional imaging capability and the high-penetration of infrared light

makes it particularly suitable for imaging of thick specimens [7, 8]. The achieved resolutions and the contrast between anatomic features are higher than for other optical modalities like confocal reflectance microscopy or optical coherence tomography [9]. Furthermore, MPT can be straightforwardly combined with fluorescence lifetime imaging (FLIM), where the signal lifetime is depicted with spatial resolution [8, 10], second harmonic imaging (SHG) [11], which can help to clearly identify dermal collagen and correlate it with the abundance of elastin [12, 13], and further modalities, e.g., non-linear Raman imaging [14, 15]. MPT devices for skin imaging typically rely on laser- scanning setups which, on the one hand, offer fast imaging, but on the other hand, provide in one frame horizontal (xy) optical sections only [6, 8, 15]. In contrast, the microscopic images of histological samples with which pathologists are trained depict vertical (xz) sections [1]. A direct comparison regarding the usefulness for diagnosis between in vivo optical biopsies and histopathology is difficult and maybe confusing because of the different image orientations which go along or perpendicular to the anatomic skin layers [16]. In this paper, typical MPT images of in vivo human skin are discussed and compared to histopathological skin images from the literature. We have adjusted a clinical MPT to record vertical optical skin biopsies, i.e., image information which are otherwise only obtained from histopathology directly, in vivo at significantly reduced time and cost expanses. Furthermore, by combining horizontal, vertical and FLIM imaging for both orientations of human skin in vivo not only the potential for microscopic skin imaging of the epidermis and upper dermis is illustrated, but also anatomic characteristics like the thicknesses of the stratum corneum and epidermis can be easily derived and analyzed. The discussion treats healthy skin only, nonetheless, a future extension to different kinds of diseased skin as well as effects of topically applied substances and penetration studies is obvious [17-19].

3. Materials and Method

3.1 Multiphoton Imaging

All MPT images presented here were recorded with a multiphoton tomograph MPTflex (JenLab GmbH, Berlin, Germany) outfitted with a modified scan-detector head which allows for direct vertical and horizontal image recording. The MPTflex is a CE certified tomograph for *in vivo* clinical imaging of human skin and ex vivo tissue imaging [15]. It is a mobile system which incorporates a tunable femtosecond laser (MaiTai XF, Newport Spectra Physics, pulse duration ~100 fs, repetition rate 80 MHz, tuning range 710-920 nm), control electronics, optical power control, safety features and a scan-detector head which is hold by an articulated arm in one housing (Figure. 1). For the MPT images shown throughout the paper, a wavelength of 760 nm was chosen and laser powers between 7-30 mW were applied at the skin. The laser pulses were focused onto the sample with a high-NA microscope objective (Zeiss EC, plan neofluar 40x/1.30 oil). Signal photons were collected in reflection geometry by the same objective. Collected signals were simultaneously recorded in two spectral channels by photomultiplier tubes in a non-descanned setup. Channel 1 and 2 comprised the wavelength ranges between 407 nm and 680 nm and between 373 nm and 387 nm, thereby, separating endogenous skin fluorescence and SHG signals, respectively. The imaging of the skin was performed on the left forearms of female and male volunteers according to a procedure described previously [20], i.e., by attachment of a magnetic metal ring onto the skin onto which the scan-detector head couples. The experimentally determined lateral and axial resolutions were (0.39 ± 0.02) µm and (1.85± 0.15) µm, respectively [15]. The scan-detector head allowed to move the microscope objective in z direction by a stepper motor and synchronize the positioning with either the x (y) directional scanning mirror such that xz (yz) images could be directly generated: whenever the scanning mirror completed an x- (or y-) line scan, the distance was changed such that the next line scan started at a different image row. With each step of the z motor, the objective was moved by 0.82 µm. The maximum travel range along z was 5 mm [17]. The duration to record an xz image with 512 x 200 pixels (255 µm x 100 µm) was about 20 s. To record FLIM images, time-correlated single photon counting (TCSPC) with a temporal resolution of about 170 ps was employed in the system [10]. FLIM images were obtained by pseudo-color coding of the mean-fluorescence decay time values which were obtained from pixelwise fitting a two-exponential decay curve to the fluorescence data. The mean fluorescence-decay time taum=a1tau1+a2tau2 was calculated from the decay-time fitting parameters tau1, tau2 and the associated normalized amplitudes a1, 2 [10].

3.2. Histopathologic Images

The histopathological images were taken from a publication by [21]. The authors obtained human abdominal skin samples from three healthy females after plastic surgery from the Division of Plastic Surgery and Hand Surgery, Helios Clinic Emil von Behring, Berlin, Germany. Details about the sample preparation, staining and imaging procedures can be found in the publication. Briefly, the skin samples were embedded in paraffin blocks and sectioned at a thickness of 5 µm with a microtome, hence, the slices consisted of thin vertical skin sections. Different staining procedures were applied: standard hematoxylin and eosin staining procedures as well as protocols according to Richardson and Volkmann-Strauss in order to visualize collagen and elastic fibers [1, 21, 22]. Images were recorded with a light microscope and a digital camera.

4. Results and Discussion

4.1 Ex Vivo Histological vs. *In Vivo* Multiphoton Skin Images

In the following, ex vivo light microscopy and in vivo MPT images of stained and unstained healthy human skin sections are discussed. Figure 2 shows skin samples histologically prepared ac-

cording to different standard staining protocols: hematoxylin and eosin (HE) staining, staining according to Richardson and staining according to Volkmann-Strauss. The images (Figure 2 a-c) depict the epidermal layers (stratum basale, stratum spinosum, stratum granulosum and stratum corneum) as well as parts of the upper dermis (Fig. 2 a, c). The ex vivo tissue staining allows a qualitative interpretation of cell morphology and tissue architecture. However, different staining procedures that highlight different parts of the skin are required to provide complementary information. It is also important to notice that each section can only be stained following one staining protocol. Therefore, complementary information is obtained in adjacent areas of the tissue rather than for same area. In HE staining (Figure. 2 a), hematoxylin dyes the cellular nuclei blue, while eosin dyes the non-nuclear cells and structures pink/orange, such as cytoplasm and collagen. A clear identification of the dermal network of collagenous and elastic fibers is achieved by Volkmann-Strauss staining (Figure 2 c). The dermo-epidermal junction can be clearly distinguished with both HE as well as Volkmann-Strauss staining. The Richardson staining is considered to provide in many cases the best representation of nuclear and cytoplasmic detail [23]. In addition to the visualization of the skin structure and its components, quantitative analysis is possible. This includes (e.g., as performed by [5] (I) the measurements of the thicknesses of the epidermis as well as of each stratum of the epidermis (stratum basale, spinosum, granulosum, corneum), (II) counting the numbers of layers of each epidermal stratum, (III) measurement of the thickness of the dermis, (IV) calculation of the dermal epidermal thickness ratio, and (V) the measurement of the length of the dermo- epidermal interface. Furthermore, peculiar skin characteristics like the number of sweat glands, hair follicles, arrector pili muscles as well as blood vessels can be counted and the area of dermis measured [5]. Although, the histologically prepared section provides valuable and detailed information, the preparation procedures also introduce typical artifacts that do not correspond to the situation of living tissue. For example, the stratum corneum in Figure 2 a) and c) is partially disrupted and appears lacy or frayed in other parts. This appearance is an artifact of the sectioning. Also, a compression or extension of parts of a skin section often occurs which leads to a loss of the compactness and connectivity compared to living tissue. To exemplify the MPT imaging capability for in vivo skin, Figure 3 depicts a vertical and eight horizontal optical sections from different depths. No staining procedure was necessary since the image signals stem from several endogenous fluorophores like keratin, NAD (P) H, flavins, melanin, collagen, and elastin which are contained in the skin in different abundancies [6]. In addition, SHG signals stem from the light-tissue interaction with collagen fibers. The images provide simultaneously detailed information on the microscopic anatomy of the skin layers. Epidermal cells and dermal collagen and elastic fibers network. In the vertical image (Figure 3a), the threefold separation of the anatomic skin layers of the epidermis and upper dermis can be immediately recognized: the stratum corneum as a bright structureless layer, the cell-containing layers (stratum granulosum, stratum spinosum, stratum basale) with discernable cellular structures and cell nuclei, and the elastin-collagen network of the upper dermis which appears mainly in red due to the strong collagen-SHG signals. In Figure 3 b), horizontal optical sectioning at different depths is depicted. The images show detailed cellular structures, skin morphology, and the beginning of the collagen-elastin fiber network in the stratum papilare starting at a depth of 35 µm. The horizontal images provide features in even higher detail than in the vertical image due to fact that the lateral resolution is higher than the axial resolution. In contrast to the histopathologic images (Figure 2), MPT images can be recorded *in vivo* in seconds or tens of second seconds. It also easily possible to record a vertical image at a slightly shifted position which may be of interest to determine the boundary of a specific skin lesion. In a histopathological examination, this would require the preparation, staining and investigation of a different microtome section. With MPT in vivo imaging, this can be easily and quickly realized by tuning to a different y position before the xz recording. This illustrates Figure 4, which shows xz-MPT-intensity images recorded at different, but fixed, y positions and in addition corresponding FLIM images. In both types of images, (intensity and lifetime images), the epidermis (indicated by I and II) and the dermis (III) are clearly distinguishable. The stratum corneum (I) appears as a bright thin layer and is discernable from the epidermal layers below which contain living cells. The presence of the main fluorophores (e.g. keratin, NAD(P)H, FAD, melanin, elastin, and collagen) can be confirmed by comparing the observed decay-time values with known literature data. The mainly blue and green colored region in the stratum corneum represent mean decay times between approximately 0.5 ns and 1.0 ns which can be attributed to keratin. Below the stratum corneum, a dark line with only weak fluoresce may indicate transition to the cell- containing region (II). This region can be further separated by overall longer decay times above (region IIa) and overall shorter decay times below (region IIb) visible by the yellow-orange coloring. Region IIa has mean fluorescence decay times between approximately 0.5 ns and 1.0 ns can be attributed to living cells (keratocytes) with NAD (P) H being the main fluorophore. The shorter fluorescence decay times in region IIb indicate the presence of melanocytes with very fast decaying fluorescence of melanin [3, 6]. The mean decay times at depth >60 µm (region III) reflect the values of elastin and collagen. The xz images also allow to track the courses of morphological features. For example, anatomic peculiarities below a skin wrinkle, which appears as a channel-like structure in the xy image (Figure 4 right), can be followed into the skin. The wrinkle (position B in the xz images) is only approximately 15 µm deep. The xz images reveal how the skin composition below the wrinkle is affected throughout the imaged depth by a thickened stratum

corneum and bent-down layers below. The MPT images allow a similar quantitative analysis of some skin characteristics as mentioned above for the histological sections. For example, by image analysis it is straightforward to derive from the imaged skin sections thicknesses of stratum corneum and epidermis of (10±2) µm and (55±5) µm. Other characteristics, however, like the thickness of the dermis or the dermal-epidermal thickness ratio cannot be derived because the maximum MPT imaging depth is not sufficient through the whole dermis.

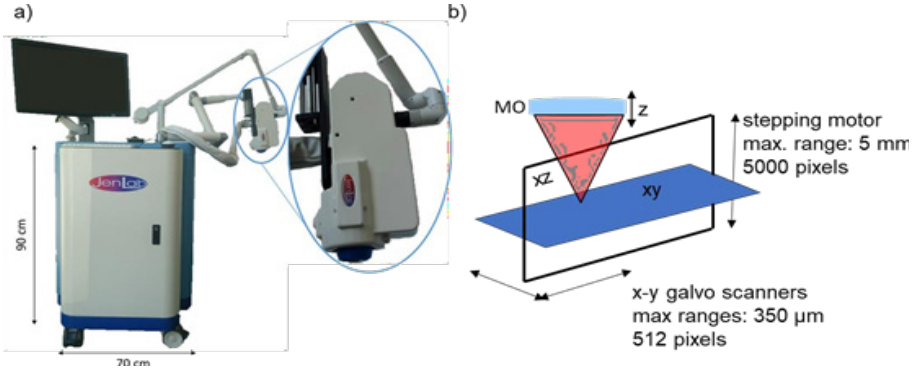

Figure 1 a: Multiphoton tomograph for direct xy, xz and yz imaging. b) Direct vertical imaging is achieved by synchronizing the movements of a galvanometer scanning mirror for beam steering and a stepper motor to control the relative microscope objective (MO) -to- sample height.

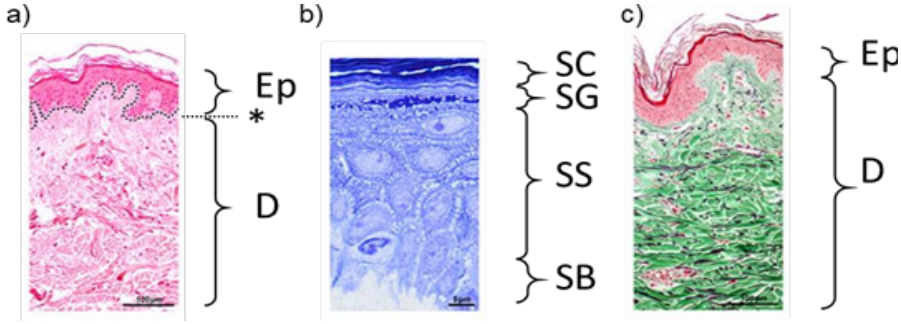

Figure 2: Light microscopy images of histology samples of human abdominal skin prepared according to different staining procedures. a) hematoxylin and eosin staining, scale bar 100 µm; Ep, epidermis; D, dermis; asterix (*), dermo-epidermal interface line. b) Staining according to Richardson, scale bar 5 µm; SC, *stratum corneum*; SG, *stratum* granulosum; SS, *stratum* spinosum; SB, *stratum basale*. c) Staining according to Volkmann-Strauss, scale bar 100 µm; Ep, epidermis (red); D, dermis with collagenous fibers (green) and elastic fibers (dark purple). The images are adapted from Ref. [21].

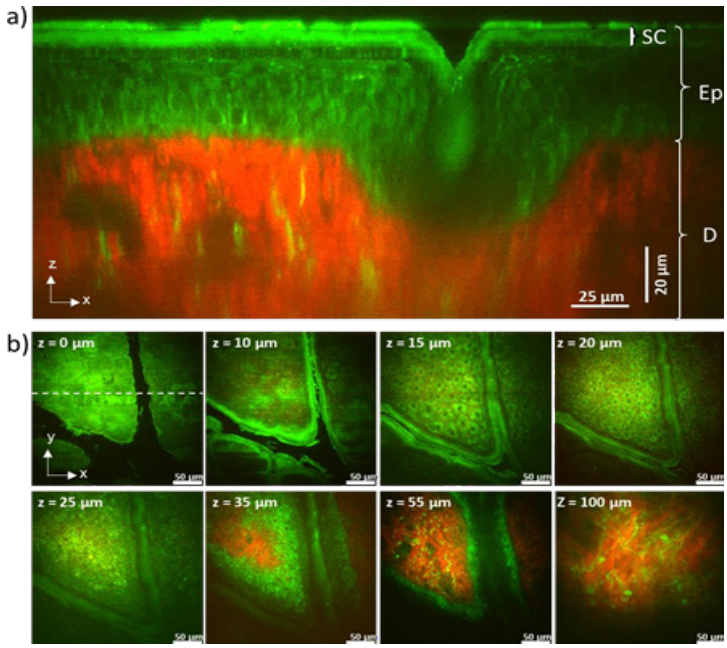

Figure 3: MPT intensity imaging of human skin *in vivo*. Green and red depict endogenous fluorescence and SHG signals, respectively. a) Vertical xz image. SC: *stratum corneum*, Ep: epidermis, D: dermis. b) Horizontal xy images from an area that includes the section depicted in a) at different depths. The dashed line indicates the position of the xz image.

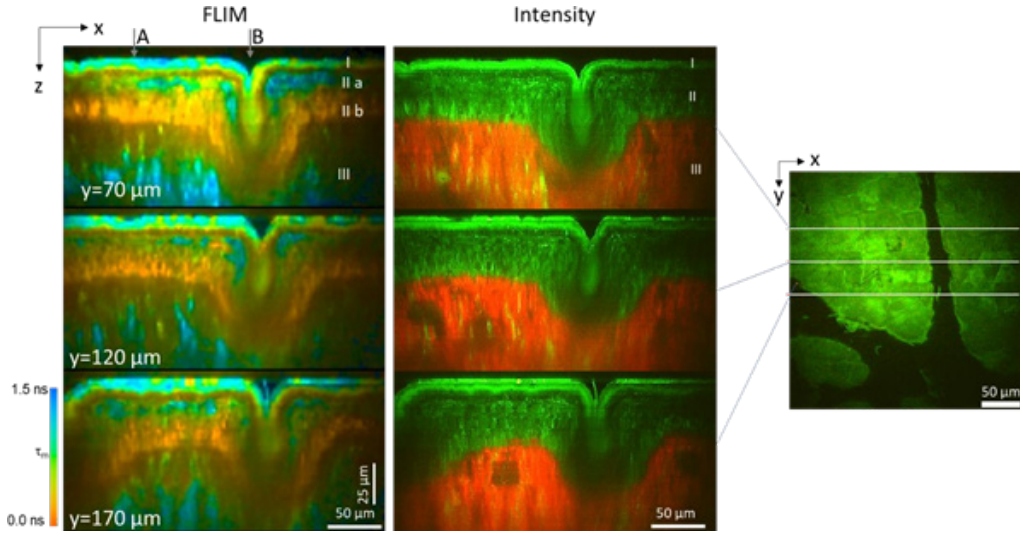

Figure 4. Vertical (xz) FLIM and intensity MPT images of human skin *in vivo* recorded with lateral separations of 50 µm. The positions of the vertical images are indicated in the xy image on the right side which provides a "view from the top".

4.2. Depth Dependence of *In Vivo* Multiphoton Signals

Both intensity and FLIM data can also be used to investigate depth dependent curves and easily derive data on the microscopic skin morphology. This is exemplified in the following. Figure 5 a) shows the depth-resolved intensity through the xy image (Figure 4) at the positions A and B. With increasing depth, the AF intensity signal at position A is highest at the surface, decreases then rapidly, exhibits a local maximum and subsequently drops. The curve reflects roughly the abundance of fluorescent molecules and inside the skin layers but is not corrected for effects like scattering and absorption of both laser and signal photons which become increasingly important with increasing depth. The SHG curves start at a low signal level and strongly increase with depth as the collagen containing upper dermis is reached. The SHG signal curve at position A exhibits local maxima and minima which reflect the microscopic dermal structure. Both signals (at positions A and B) eventually decrease as a result of both absorption and scattering of backscattered SHG photons and incoming excitation light by the above laying tissue. While the specific depth values differ by individual skin characteristics of the imaged person, the described trends of the curves are quite general, which enables quick automatic skin sectioning [12]. This can be supplemented by depth-resolved taum curves (Fig. 5b) which also indicate the different anatomic layers as well the changes of types and abundancies of fluorophores. For line A, values >500 ps agree with values reported in the literature for keratin [24]. A subsequent minimum of the curve results from the presence of NAD (P) H-containing keratinocytes. With further depth, the abundance of melanin, which has a short fluorescence lifetime, increases in the stratum basale. The subsequent increase of taum values for depths >60 µm reflects the increasing abundance of elastin and collagen fibers inside the dermis with longer fluorescence decay times. The T_m curve at position B shows two distinct minima indicating a different (or at least "shifted") fluorophore composition below the skin wrinkle compared to the position A. The characteristic shape of the T_m curves can be straight forwardly used to easily derive the thicknesses of the stratum corneum and the epidermis along the cross section by determining the positions of the two minima. Fig. 6 shows examples of the normalized T_m-depth dependence from different volunteers recorded at different positions on the forearm and averaged in each case over six xz images from different skin regions. The general trend of the depth dependence of taum, i.e., a sharp local and a shallower absolute minimum which indicate the beginning and end of the stratum corneum and the epidermis, respectively, is present in all curves. It reflects the general human skin anatomy. The distinctive pattern can be used to easily and robustly determine the microscopic thickness of the stratum corneum as well as the epidermis by straightforward determination of the minima in the T_m curves. Both are often looked-after values for medical skin diagnostics and evaluation of cosmetics.

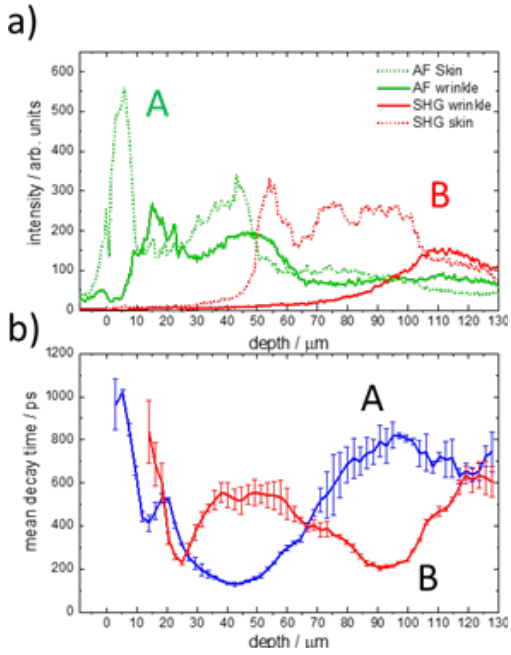

Figure 5. Depth dependence of (a) intensity and (b) lifetime values from the xz images shown in Figure 4 obtained at positions A and B.

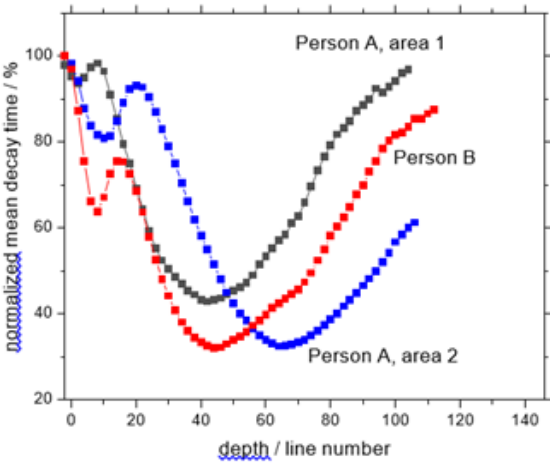

Figure 6. Depth dependence of lifetime values from two different persons.

5. Conclusion

Although histopathologically prepared sections remain the gold standard for the diagnosis of skin conditions due to their high contrast and highly detailed image information, sample preparation and staining is demanding and time consuming. Vertical optical sections by MPT provide several features of the skin within a few seconds to a few minutes. So far often-different image geometries, i.e., vertical versus horizontal sectioning hindered direct comparison between ex vivo histological sections and in vivo MPT images. We modified the conventional horizontal scanning procedure of a clinical MP tomograph by synchronizing horizontal line scans with tuning of the imaging depth to directly record xz images. The combination of xz and conventional xy images allows a fast identification of different anatomic skin layers and their microscopic features in vivo similar to what can be obtained from histological sections ex vivo. Future applications of vertical MPT imaging include direct evaluation of substance penetration into the skin and fast evaluation of skin conditions *in vivo*.

6. Acknowledgements

This project has received funding from EUREKA under the Eurostars program (grant agreement number E!10689 FLIM-VERTICO).

References

1. C E Day. Histopathology: Methods and protocols. 2014.
2. M Mogensen, G B Jemec. Diagnosis of nonmelanoma skin cancer/keratinocyte carcinoma: a review of diagnostic accuracy of nonmelanoma skin cancer diagnostic tests and technologies. Dermatologic Surgery. 2007: 33(10); 1158-1174 (2007).
3. E Dimitrow, et al. “Spectral fluorescence lifetime detection and selective melanin imaging by multiphoton laser tomography for melanoma diagnosis,” Experimental dermatology. 2009; 18(6): 509-515.
4. A Brozyna, B W Chwirot. “Porcine Skin as a Model System for Studies of Ultraviolet a Effects in Human Skin,” Journal of Toxicology and Environmental Health, Part A. 2006; 69(12): 1155-1165.
5. M E Darvin, et al. “Comparison of in vivo and ex vivo laser scanning microscopy and multiphoton tomography application for human and porcine skin imaging,” Quantum Electronics. 2014; 44(7): 646-651.
6. K König. “Clinical multiphoton tomography,” J Biophotonics. 2008; 1(1): 13-23.
7. W R Zipfel, R M Williams, WW Webb. “Nonlinear magic: multiphoton microscopy in the biosciences,” Nat Biotechnol. 2003; 21(11): 1369-77.
8. K König, T Baldeweck, M Balu. Multiphoton Microscopy and Fluorescence Lifetime Imaging] De Gruyter. 2018.
9. K König, M Speicher, R Bückle. “Clinical optical coherence tomography combined with multiphoton tomography of patients with skin diseases,” J Biophotonics. 2009; 2(6-7): 389-397.
10. K Suhling, LM Hirvonen, JA Levitt. “Fluorescence lifetime imaging (FLIM): Basic concepts and some recent developments,” Medical Photonics. 2015; 27: 3-40. R Cicchi, N Vogler, D Kapsokalyvas. “From molecular structure to tissue architecture: collagen organization probed by SHG microscopy,” Journal of Biophotonics. 2013; 6(2): 129-142.
11. A Schindele, H G Breunig, K König. “Multiphoton Tomography for in Vivo Skin Age Determination: Dermal autofluorescence and second harmonic generation allow non-invasive imaging of biological tissue,” Optik & Photonik. 2018; 13(2): 56-59.
12. MJ Koehler et al. “Morphological skin ageing criteria by multiphoton laser scanning tomography: non-invasive in vivo scoring of the dermal fibre network” Exp Dermatol. 2008; 17(6): 519-23.
13. H G Breunig, et al. “Clinical coherent anti-Stokes Raman scattering and multiphoton tomography of human skin with a femtosecond laser and photonic crystal fiber,” Laser Physics Letters.2013; 10(2).
14. M Weinigel, et al. “Multipurpose nonlinear optical imaging system

for in vivo and ex vivo multimodal histology," J Med Imaging (Bellingham). 2015; 2(1): 016003.

15. P A Kolarsick, MA Kolarsick, C Goodwin. "Anatomy and physiology of the skin," Journal of the Dermatology Nurses' Association. 2011; 3(4): 203-213.
16. HG Breunig et al. "Rapid vertical tissue imaging with clinical multiphoton tomography" SPIE-Proceed.2018;106790N.
17. Weinigel et al. "In Vivo Imaging of ZnO Nanoparticles from Sunscreen on Human Skin with a Mobile Multiphoton Tomograph," BioNanoScience. 2015; 5(1): 42-47.
18. K König, AP Raphael, L Lin. "Applications of multiphoton tomographs and femtosecond laser nanoprocessing microscopes in drug delivery research," Adv Drug Deliv Rev. 2011; 63(4-5): 388-404.
19. Breunig et al. "Multiphoton excitation characteristics of cellular fluorophores of human skin in vivo," Optics Express. 2010; 18(8): 7857-7871.
20. M Khiao In, K C Richardson, A Loewa. "Histological and functional comparisons of four anatomical regions of porcine skin with human abdominal skin," Anat Histol Embryol. 2019; 48(3): 207-217.
21. K Richardson, L Jarett, E Finke. "Embedding in epoxy resins for ultrathin sectioning in electron microscopy," Stain technology. 1960; 35(6): 313-323.
22. A Chu, N Smith, D MacDonald. "Evaluation of staining methods for resin embedded cutaneous tissue sections of mycosis fungoides," British Journal of Dermatology. 1980; 103(6): 607-614.
23. J A Palero, H S de Bruijn, A van der Ploeg van den Heuvel. "Spectrally resolved multiphoton imaging of in vivo and excised mouse skin tissues," Biophys J. 2007; 93(3): 992-1007.